JACS
JOURNAL OF THE AMERICAN CHEMICAL SOCIETY
Article
pubs.acs.org/JACS

Two-Photon-Pumped Perovskite Semiconductor Nanocrystal Lasers

Yanqing Xu,[†,§] Qi Chen,[†,§] Chunfeng Zhang,[*,†,‡] Rui Wang,[†] Hua Wu,[∥] Xiaoyu Zhang,[∥] Guichuan Xing,[⊥] William W. Yu,[∥] Xiaoyong Wang,[†] Yu Zhang,[*,∥] and Min Xiao[*,†,‡,#]

[†]National Laboratory of Solid State Microstructures, School of Physics, and Collaborative Innovation Center of Advanced Microstructures, Nanjing University, Nanjing 210093, China

[‡]Synergetic Innovation Center in Quantum Information and Quantum Physics, University of Science and Technology of China, Hefei, Anhui 230026, China

[∥]State Key Laboratory on Integrated Optoelectronics and College of Electronic Science and Engineering, Jilin University, Changchun 130012, China

[⊥]Key Laboratory of Flexible Electronics & Institute of Advanced Materials, Jiangsu National Synergistic Innovation Center for Advanced Materials, Nanjing Tech University, 30 South Puzhu Road, Nanjing 211816, P.R. China

[#]Department of Physics, University of Arkansas, Fayetteville, Arkansas 72701, United States

Supporting Information

ABSTRACT: Two-photon-pumped lasers have been regarded as a promising strategy to achieve frequency up-conversion for situations where the condition of phase matching required by conventional approaches cannot be fulfilled. However, their practical applications have been hindered by the lack of materials holding both efficient two-photon absorption and ease of achieving population inversion. Here, we show that this challenge can be tackled by employing colloidal nanocrystals of perovskite semiconductors. We observe highly efficient two-photon absorption (with a cross section of 2.7×10^6 GM) in toluene solutions of $CsPbBr_3$ nanocrystals that can excite large optical gain (>500 cm^{-1}) in thin films. We have succeeded in demonstrating stable two-photon-pumped lasing at a remarkable low threshold by coupling $CsPbBr_3$ nanocrystals with microtubule resonators. Our findings suggest perovskite nanocrystals can be used as excellent gain medium for high-performance frequency-up-conversion lasers toward practical applications.

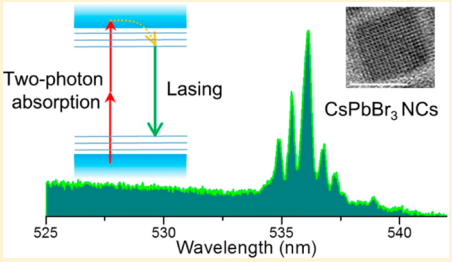

INTRODUCTION

Visible lasing achieved with infrared multiphoton pumping has been proposed as an alternative approach for frequency up-conversion,[1−13] which is viable for applications of three-dimensional material fabrication and biomedical photonics owing to the merits of spatially confined excitation and no phase-matching requirement.[1,14,15] However, such new type of lasers have strict demands on the optical properties of the gain media, i.e. large optical gain with highly efficient multiphoton absorption, which limit the available lasing materials to certain selective organic dyes,[1−4] polymers,[13] and inorganic semiconductor nanostructures.[5−11,16] Among those applicable systems, zero-dimensional CdSe nanocrystals (NCs) exhibit excellent performances[6−8,10,11,16] benefiting from the high photoluminescence (PL) efficiency (>80%)[17,18] and a relatively large cross section of two-photon absorption (10^3−10^4 GM, 1 GM = 10^{-50} cm^4 s).[19,20] Nevertheless, efficient two-photon-pumped optical gain in CdSe NCs can only be achieved when the pumping power exceeds a relatively high threshold value (typically, >5 mJ cm^{-2}).[6,7,9−11]

Recently, perovskite lead halide semiconductors have emerged as an excellent family of materials for optoelectronic applications which have attracted tremendous attention for their exceptional performances in solar cells and photodetectors.[21−28] This new class of semiconductors have low density of midgap trap states,[29] long carrier diffusion length,[30−32] and high PL efficiency,[33] making them also promising for applications in light-emitting diodes and lasers.[16,21,33−37] Colloidal nanostructures of perovskite semiconductors have recently been synthesized to further promote their light-emitting performance by the aid of the quantum confinement effect.[38−47] Notably, the amplified spontaneous emission (ASE) and lasing from NCs of cesium lead halide ($CsPbX_3$, X= Cl, Br, and I) have recently been demonstrated with a low threshold under one-photon pumping.[45] In comparison to the conventional CdSe NCs, the absorption cross section of $CsPbX_3$ NCs is about 2 orders of magnitude larger, indicating strong light−matter interaction in the perovskite semiconductor NCs.[45,48] The emission color can be tuned with a simple procedure of anion exchange without modifying the size-dependent properties,[40,42] making $CsPbX_3$ NCs particularly suitable for color-tuning applications.

Received: December 4, 2015
Published: March 3, 2016

DOI: 10.1021/jacs.5b12662
J. Am. Chem. Soc. 2016, 138, 3761−3768

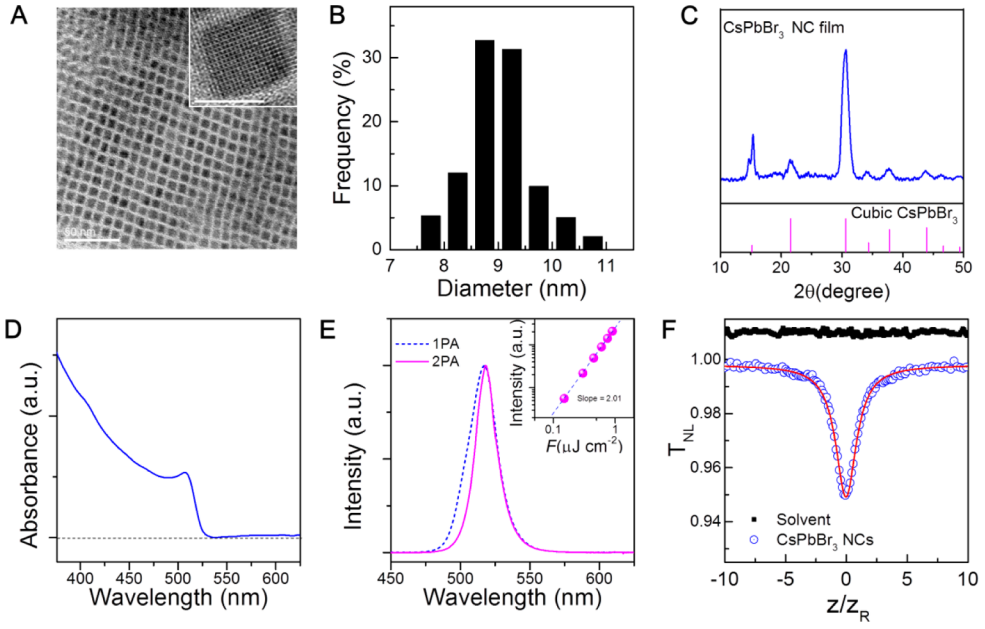

Figure 1. Two-photon absorption of $CsPbBr_3$ NCs. (A) TEM images of CsPbBr3 NCs. The inset shows a high-resolution TEM image of a single NC. (B) Histogram for the size distribution of $CsPbBr_3$ NCs. (C) Experimental XRD spectrum (top) of a $CsPbBr_3$ NC film and standard XRD patterns (bottom) for the cubic phases of $CsPbBr_3$. (D) Linear optical absorption spectrum of a typical NC film. (E) Normalized PL spectra recorded under one-photon and two-photon excitations recorded from a drop-cast film, respectively. The inset shows the quadratic dependence of PL emission on the fluence of two-photon excitation. (F) The open aperture z-scan curve measured on the toluene solution of $CsPbBr_3$ NCs.

In this paper, we report the feasibility of using perovskite semiconductor NCs to tackle current challenges facing the two-photon-pumped lasers. In a model system of $CsPbBr_3$ NCs, we have observed a large cross section of two-photon absorption at 800 nm (~2.7×10^6 GM). Two-photon-pumped optical gain is explicitly observed by employing ultrafast transient absorption (TA) spectroscopy, which can support ASE in $CsPbBr_3$ NC films with a remarkable low threshold value (~0.8 mJ cm^{-2}). With variable stripe length (VSL) measurements, a large modal gain coefficient (>500 cm^{-1}) in the frequency up-converted domain has been observed in $CsPbBr_3$ NC films. By incorporating the optical gain in microcapillary resonators, we have successfully demonstrated whispering gallery (WG) mode lasing under two-photon pumping with perovskite $CsPbBr_3$ NCs. The realized perovskite NC lasers with remarkable high modal gain under ambient conditions suggest that perovskite NCs can be excellent candidates for two-photon-pumped lasers toward practical applications.

EXPERIMENTAL SECTION

Sample preparation. Colloidal $CsPbBr_3$ NCs were synthesized with an approach[48] modified from the one-step technique developed by Kovalenko and co-workers.[38] The purified NCs were dispersed in toluene solvent with the density of NCs carefully calibrated (For details, see Supporting Information (SI)). Quantum efficiency of PL emission is above 60% as characterized with an integrating sphere.[49] The NC sample has been characterized by transmission electron microscopy (TEM) and X-ray diffraction (XRD). A quartz cuvette (0.1 mm thick) filled by toluene solution of $CsPbBr_3$ NCs (2 μM) was employed for z-scan measurement. For TA spectroscopic experiments, thin NC films were fabricated by spin coating with thickness controlled by spinning rate and solution concentration. To demonstrate ASE, thick films of $CsPbBr_3$ NCs were prepared by drop-casting $CsPbBr_3$ NCs on glass substrates. Thicknesses of the NC films were checked by profilometer. The system of gain media coupled to microcavity resonators are formed by drawing concentrated toluene solutions of NCs into microcapillary tubes. The samples were left in vacuum overnight to evaporate the solvent. More details are available in SI.

Optical characterizations. The standard optical characterizations for steady optical properties of the prepared samples are described in SI. For TA spectroscopy, pump pulses at 800 nm (Libra, Coherent, 1 kHz, 90 fs) generate the two-photon excitations in the NC films. The carrier dynamics was probed by a broadband supercontinuum light source that was generated by focusing a small portion of the femtosecond laser beam onto a sapphire plate. The chirp of the probe supercontinuum was corrected with error to be less than 100 fs over the whole spectral range. The TA signal was then analyzed by a high-speed charge-coupled device (S11071-1104, Hamamatsu) with a monochromator (Acton 2358, Princeton Instrument) at 1 kHz enabled by a custom-built board from Entwicklungsbuero Stresing. The signal-to-noise ratio in differential transmission is better than 5 $x10^{-5}$ after accumulating and averaging 1,000 pump-on and pump-off shots for each data point. The angle between the polarizations of pump and probe beam was set at the magic angle. The ASE and lasing characterizations were performed with two-photon excitations by femtosecond pulses at 800 nm from a Ti:sapphire regenerative amplifier (Libra, Coherent, 1 kHz, 90 fs) under ambient environment. For VSL measurements, the beam was focused into a stripe by a cylindrical lens with a focal length of 10 cm. To demonstrate lasing, the emission from the NC-implanted microcapillary tube was collected normal to the tube with an objective lens. The emission was then routed to a monochromator (Acton 2500i, Princeton Instrument) and analyzed with a liquid-nitrogen-cooled charge-coupled device with spectral resolution of 0.1 nm.

RESULTS AND DISCUSSION

Figure 1A shows the morphology of $CsPbBr_3$ NCs characterized by TEM. The sizes of the cubic shaped NCs are estimated to be 9 ± 1 nm by TEM (Figure 1B). This size is comparable to the excitonic Bohr radius (~7 nm)[38] and results in a clear quantum confinement effect, as evidenced by the bandgap offset and the recent demonstrations of single-photon emission from single $CsPbBr_3$ NCs.[48,50] $CsPbBr_3$ NCs exhibit cubic structure at room temperature, as characterized by high-

DOI: 10.1021/jacs.5b12662
J. Am. Chem. Soc. 2016, 138, 3761−3768

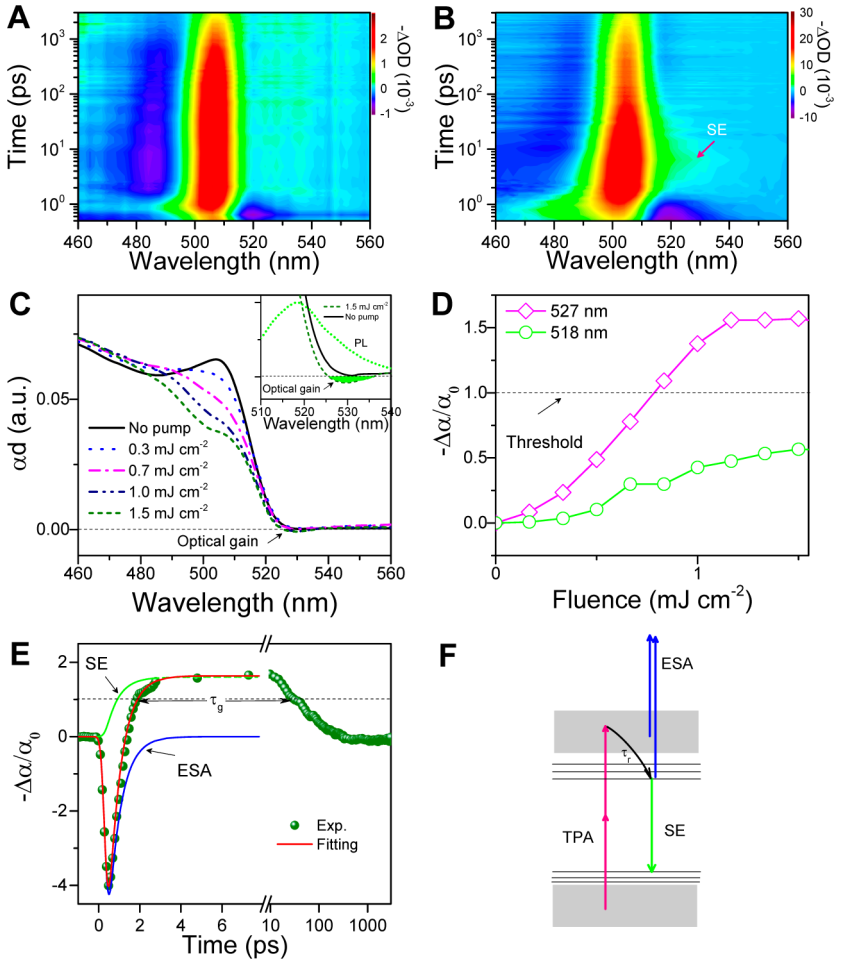

Figure 2. TA study of optical gain with two-photon excitation. (A, B) TA spectroscopic data of a NC film with two-photon excitation at 0.3 and 1.5 mJ cm^{-2}, respectively. The SE feature is manifested as a pronounced bleach signal with high fluence pumping (B). (C) Development of optical gain in pump-dependent nonlinear absorption spectra recorded at a delay time of ~5 ps. Inset: a magnified view of the spectroscopic signature of optical gain pumped by two-photon excitation. (D) Pump-fluence-dependent nonlinear absorption changes ($-\text{-}\Delta\alpha/\alpha_0$) measured at 518 nm, and 527 nm, respectively. (E) The TA kinetics probed at 527 nm consists of the components of SE and ESA with two-photon excitation at 1.5 mJ cm^{-2}. The dashed line indicates the gain threshold. The lifetime with gain above the loss is labeled as τ_g = 35 ps. (F) Schematic diagram of the mechanism of optical gain with two-photon excitation.

resolution TEM (Inset, Figure 1A) and X-ray diffraction (Figure 1C). The excitonic absorption spectrum shows a narrow excitonic peak at 505 nm (Figure 1D). The cross section of linear absorption at 400 nm ($\sigma^{(1)}$) is evaluated to be ~1.2×10^{-13} cm^{-2} (Details are available in SI). The excitonic PL emission can be generated under either one-photon or two-photon excitation. Figure 1E compares the normalized PL spectra recorded from a drop-cast film with pulse excitations at 400 and 800 nm, respectively. The PL intensity excited at 800 nm shows a quadratic power dependence when the excitation fluence is relatively low (Inset, Figure 1E), confirming two-photon absorption to be the primary excitation pathway. The PL emission excited at 800 nm is on the red side of PL excited at 400 nm with a slightly longer decay lifetime (Figure S4, SI). Such a redshift was typically ascribed as due to the reabsorption effect in single crystals of $CH_3NH_3PbI_3$.[51] Nevertheless, the reabsorption effect in thin films should not be as significant as that in single crystals. Other factors with divergent relaxation pathways relevant to different selection rules for one- and two-photon excitation processes may be involved, which deserves in-depth study in the future.

Figure 1F presents a z-scan curve measured on the sample of toluene solution of $CsPbBr_3$ NCs with a peak intensity of 100 GW/cm^2 together with the control experiment on the solvent itself. A thin quartz cuvette (0.1 mm thickness) was chosen to satisfy the widely-used approximation established by Sheikbahae et al. [Details available in SI].[52] The cross section of two-photon absorption ($\sigma^{(2)}$) is estimated to be ~$2.7 \pm 1.0 \times 10^6$ GM at 800 nm in $CsPbBr_3$ NCs, which is further confirmed by directly measuring the power-dependent nonlinear transmission on solutions (Figure S2, SI) and z-scan experiments on films (Figure S1, SI). This value is over two-orders of magnitude larger than that of the CdSe NCs emitting similar color [Figure S3A, SI].[6,7] Recently, the two-photon absorption coefficient in bulk crystals of $CH_3NH_3PbBr_3$ was found to be comparable to that in bulk CdS semiconductor.[53] The value in $CsPbBr_3$ NCs, if scaled in volume, is much higher than $CH_3NH_3PbBr_3$ crystal. Such divergence is probably caused by the different oscillator strengths of interband transitions due to different cations in the materials of $CH_3NH_3PbBr_3$ and $CsPbBr_3$ besides the quantum size effect. The values of $\sigma^{(2)}$ in different $CsPbX_3$ NCs are also evaluated [Figure S3, SI]. With increasing excitonic absorption energy, the cross section

DOI: 10.1021/jacs.5b12662
J. Am. Chem. Soc. 2016, 138, 3761−3768

($\sigma^{(2)}$) decreases as a result of the bandgap effect.[53] The cross section per volume in $CsPbBr_3$ NCs is also one-order of magnitude higher than that of CdSe NCs [Figure S3B, SI], suggesting the volume effect is not the only effect responsible for the efficient two-photon absorption in perovskite NCs [Figure S3, SI]. Despite such a significant divergence in the cross sections of two-photon absorption for $CsPbBr_3$ and CdSe NCs, the ratio between two- and one-photon absorption cross sections in $CsPbBr_3$ NCs (at the order of 10^{-31} cm^{-2} s) is comparable to that in CdSe NCs. In another words, the origin of such large two-photon absorption should be similar to that for one-photon absorption in $CsPbBr_3$ NCs whose magnitude is about two-orders of magnitude higher than that of CdSe NCs due to the strong oscillator strength of interband transitions.[45,48]

When NCs are pumped into high-energy excited states, the optical gain becomes possible if the population inversion is built up when the relaxations to the emissive states are faster than the removal processes like Auger recombination and other recombination pathways. We employ ultrafast TA spectroscopy to track the development of optical gain in the NC film under two-photon excitation. The light amplification/attenuation of the NC film is probed with a broadband white-light supercontinuum source which is variably delayed with respect to the pump pulses. Considering the absorbance before and after two-photon excitation to be α_0 and α, optical gain is achieved when the two-photon-induced negative absorption ($-\Delta\alpha = \alpha_0 - \alpha$) becomes greater than α_0 (i.e., $-\Delta\alpha/\alpha_0 > 1$). Figures 2A and 2B plot the values of $\Delta\alpha$ probed near the band gap under weak and strong fluence excitations, respectively. Briefly, the signal of $\Delta\alpha$ consists of a major band of the ground-state bleaching (GSB) close to the excitonic absorption peak, a long-lived photoinduced absorption (PIA) feature in the short-wavelength range (<490 nm) and another short-lived PIA peak at 520 nm. The photoinduced bleaching (PIB) feature at 510–530 nm becomes profound with increasing excitation fluence, which is probably caused by stimulated emission (SE) (Figure 2B and 2C). The nonlinear absorption spectra recorded at a delay time of 5 ps show the emergence of an optical gain when excitation fluence exceeds the threshold value of ~0.7 mJ/cm^2 (Figure 2D). Notably, the optical gain appears in the wavelength range of 525–535 nm, although the bleaching signal covers a much broader wavelength range (Inset, Figure 2C). The value of $\Delta\alpha/\alpha_0$ probed at the PL center wavelength is below the gain threshold, even though the optical gain at 527 nm gets saturated with the pump fluence above 1.2 mJ cm^{-2} (Figure 2D).

Next let us analyze the temporal dynamics of optical gain for more insights. Figure 2E plots the TA signal ($-\Delta\alpha/\alpha_0$) probed at 527 nm. Upon pulse excitation, a PIA feature simultaneously appears followed by the buildup of absorption bleach in the first 10 ps. With excitation at 800 nm, the PIA signal may have contributions from the absorption of the excited states (ESA) that are populated simultaneously by two-photon excitation and/or the coherent nondegenerate two-photon absorption (i.e., simultaneous absorption of a pump photon and a probe photon). The PIA signal shows an exponential decay with a lifetime of ~0.6 ps, suggesting the PIA signature to be mainly contributed by the ESA from hot-excited states populated by two-photon excitation. We find that the onset of this TA signal can be modeled as a summation of ESA and SE components with the same lifetime parameter of ~0.6 ps (Figure 2E). The lifetime of optical gain (τ_g, i..e., gain > loss) is ~35 ps which is primarily limited by the loss level and the Auger recombination induced by the multiexciton effect [Figure S6]. The kinetics of optical gain can be summarized in Figure 2F as: Two-photon absorption pumps the electrons to the hot states which relax to the excitonic emissive states with a lifetime of ~0.6 ps. This rate is much faster than the recombination process from the emissive states, enabling the population accumulation at the emissive states responsible for the detected optical gain. It is worth noting that the population at the emissive excitonic states may also induce an absorption in the emission band, which was regarded as a major limitation preventing the development of optical gain in solutions of CdSe NCs.[54] This effect also causes a negative influence on the gain generation in $CsPbBr_3$ NCs as clearly seen in the TA data measured on the solution sample (Figure S5, SI). The ESA signal from emissive excitonic states is much more distinct in the solution sample than in the NC films (Figure S5, SI), which is probably due to the slow buildup of gain due to the low filling factor of NCs in solution.[54] Nevertheless, the SE signal is quite efficient that can overcome the ESA relevant to the excitonic states with increasing excitation fluence, manifesting as the PIB signal in both film and solution samples (Figure S5, SI).

We incorporate the optical gain in a slab waveguide to demonstrate the ASE from thick NC films. By drop-casting colloidal solutions of $CsPbBr_3$ NCs on glass substrates, films with thicknesses of 300–400 nm are made. Figure 3A shows

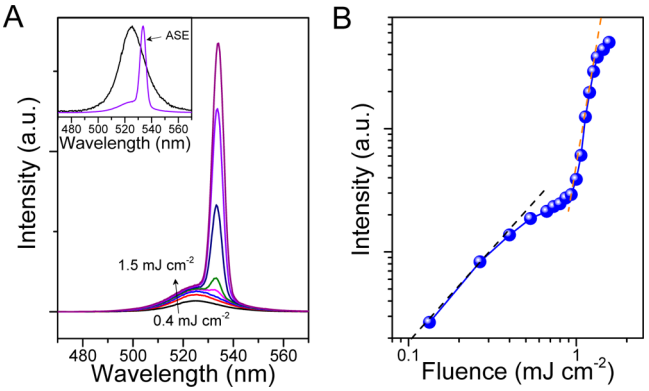

Figure 3. Two-photon-pumped ASE from $CsPbBr_3$ NC films. (A) Pump-fluence-dependent emission spectra from a $CsPbBr_3$ NC film. The inset compares the spectra of spontaneous emission and ASE in a normalized scale. (B) Pump-fluence dependence of the ASE intensity showing a threshold behavior.

the edge emission spectra recorded from a thick NC film under different fluence excitations. ASE is observed with clear evidence including the gain-induced line width narrowing (Inset, Figure 3A) and threshold behavior in power dependence of the emission intensity (Figure 3B). The peak of ASE at 533 nm is slightly red-shifted with respect to the gain revealed by ultrafast TA spectroscopy, which is probably caused by the contrast of dielectric constant in the film and solution. The threshold for ASE is ~0.8 mJ cm^{-2} which is about one-order of magnitude lower than that for CdSe NC films with similar emitting color under two-photon excitations.[6,7]

The net modal gain is a key figure-of-merit for demonstrating lasers. We evaluate optical gain using the well-established VSL method,[37,45] where the excitation beam is focused to be a strip line by a cylindrical lens whose length is controlled by an adjustable slit. Figure 4A shows the emission spectra recorded

DOI: 10.1021/jacs.5b12662
J. Am. Chem. Soc. 2016, 138, 3761–3768

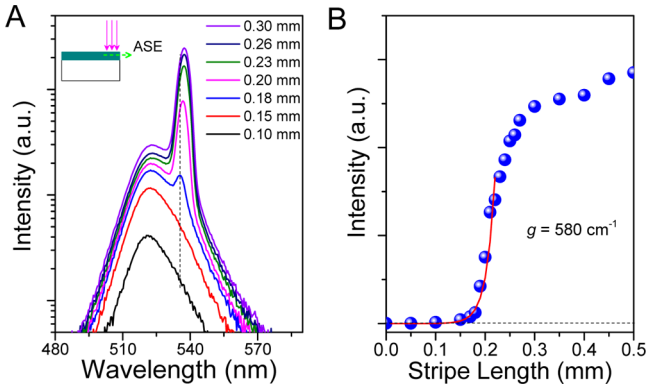

Figure 4. VSL measurements on $CsPbBr_3$ NC films. (A) Emission spectra measured with stripe lengths in the range of 0.1 to 0.30 mm. The inset shows the scheme of VSL measurement. (B) The ASE intensity is plotted as a function of stripe length.

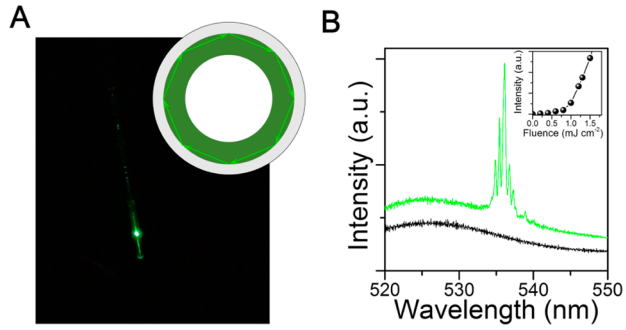

Figure 5. Two-photon-pumped microring lasing from $CsPbBr_3$ NCs. (A) Fluorescence image of a lasing cylindrical microcapillary tube incorporated with $CsPbBr_3$ NCs. Inset: the WG modes supported by the microring resonator. (B) Two-photon-pumped PL spectra recorded with excitation fluence below (0.7 mJ cm^{-2}, black) and above threshold (1.0 mJ cm^{-2}, green), respectively. The inset shows the emission intensity as a function of excitation fluence.

from a spin-cast film (~300 nm thick) with different stripe lengths under the excitation fluence of ~1.5 mJ cm^{-2}. The ASE peak emerges when the stripe length is longer than 0.16 mm, suggesting that a certain level of optical amplification is required to overcome the propagation losses. Figure 4B plots the intensity at the ASE peak as a function of the stripe length. We adopt the model describing the stripe-length-dependent ASE intensity as[45,55−59] $I = A(e^{gL} - 1)/g$, where I, G, and L are the ASE intensity, the modal gain, and the stripe length, respectively. Fitting the measured data to the model, the modal gain coefficient is then estimated to be ~580 cm^{-1} (Figure 4B). The modal gain coefficients measured in several different samples are in the range of 500−580 cm^{-1}. This is among the largest values obtained for two-photon-pumped optical gain. Recently, efficient two-photon-pumped optical gain was obtained in CdSe/ZnS nanorods and nanoplates,[8,11,12,56] in which, the cross section of linear absorption can be up to the order of 10^{13} cm^{-2},[60] suggesting that the strong light−matter interaction of linear absorption is probably also critical for achieving efficient optical gain under two-photon pumping.

Finally, we demonstrate frequency up-converted lasers by incorporating the perovskite NCs into optical resonators of glass microcapillary tubes.[55,61] The NC microcavity is fabricated by drawing toluene solution of $CsPbBr_3$ NCs into a microcapillary tube. Figure 5A displays the fluorescence image of a lasing tube showing the lasing emission leaked from the tubular sidewall. We collect the emission light normal to the tube with an objective lens and plot the spectrum integrated over 1 s (1000 excitation shots) in Figure 5B. With increasing excitation fluence, perovskite NC lasing is evidenced by sharp emission peaks with line widths of 0.15−0.3 nm (Figure 5B), indicating the quality factors of lasing modes to be in the range of 1700−3500. In principle, the high refractive index contrast between the glass tube (1.46) and NC solids (~2.30)[45] can well confine the light emission from NCs, supporting the Fabry−Perot type modes,[55] WG modes,[55,61] or random lasing action.[45] The high quality factor and evenly distributed lasing peaks are likely related to the WG modes arising from the total internal reflections at the interfaces between the inner tubular surfaces and NC solids (Inset, Figure 5A). The mode spacing is $\Delta\lambda \sim 0.65$ nm [See Figure S8 for a magnified view], which is consistent with the theoretical description of a 2D model for WG modes, i.e., $\Delta\lambda = \lambda^2/\pi n_g D$,[61] where λ,D are the emission wavelength and the inner diameter of the tube, respectively, and $n_g = n(1 - \lambda dn/nd\lambda)$ is the group refractive index [Figure S8, SI]. The power dependence of the light emission (Inset, Figure 5B) shows a threshold behavior at ~0.9 mJ cm^{-2}. Control experiments were performed on CdSe/ZnS NCs with a similar cavity design. However, the threshold for the two-photon-pumped microtubular lasers with red-emitting CdSe/ZnS NCs is ~21 mJ cm^{-2}, which is much higher than that for $CsPbBr_3$ NCs [Figure S10, SI].

High lasing threshold has been a major drawback that limits the applications of two-photon-pumped lasers. Considering the colloidal nature of perovskite NCs, we compare the measured threshold values for two-photon-pumped lasers in $CsPbBr_3$ NCs with previously demonstrated systems of cadmium chalcogenide colloidal NCs. ASE provides a benchmark for comparing different material sets on their suitability and performance for lasing applications. The demonstrated threshold for ASE pumped by two-photon excitation with $CsPbBr_3$ NC films (0.8 mJ cm^{-2}) is about one-order of magnitude lower than that for spherical CdSe NCs.[6,7] Recently, there is a rapidly growing interest in manipulating optical properties of CdSe nanocrystals with different shapes and dimensionality.[8,11,12,56,60,62] Performance improvements over spherical CdSe NCs in two-photon-pumped ASE have been achieved. Yet, the threshold of ASE in $CsPbBr_3$ NCs has shown to be 6−7 times better than that achieved in CdSe/CdS nanoplatelets[56] and 3−4 times better than that in CdSe/CdS nanorods.[8]. With further engineering the shapes, dimensionality and/or core/shell heterostructures employed in conventional NCs,[39,46,47,63] the two-photon absorption may be further enhanced for perovskite NCs, suggesting the promising potential for their two-photon-pumped laser applications.[8,10−12,60,62]

More recently (after we submitted the original manuscript), Wang et al. reported an observation of two-photon-pumped ASE in the similar material system.[64] Compared to that report, the value of $\sigma^{(2)}$ measured in our current work is over one-order of magnitude larger, resulting in a much lower lasing threshold.[64,65] Notably, the cross section of linear absorption obtained in their samples[44] is also much smaller than the values measured in our current work and in Kovalenko's work.[45] In spite of such a large divergence, the ratios between two- and one-photon absorption cross sections are actually comparable, implying that the divergence in absorption cross sections might be plausibly caused by sample diversity used in the different experiments. Spectral difference between PL under one- and

DOI: 10.1021/jacs.5b12662
J. Am. Chem. Soc. 2016, 138, 3761−3768

two-photon excitations is not distinct in the work of Wang et al.,[64] but can be clearly observed in the current work [Figure 1E]. Moreover, the gain mechanism and laser design proposed in our current work may also apply to other perovskite NC samples with comparable density of excitons.

In type-I CdSe NCs, the presence of multiple excitons in single NCs has been regarded as a prerequisite for gain generation due to the spin degeneracy of lowest excitonic states.[54] Single-exciton optical gain can be achieved by engineering materials to break the degeneracy of the emissive excited states.[58,66,67] In conventional NCs, only more than one photoexcited excitons per NC can support a detectable optical gain.[54] Theoretically, the high symmetric cubic phase of the perovskite $CsPbBr_3$ NCs may result in multifold degeneracy for the lowest excitonic transition.[68,69] However, the spin degeneracy can be lifted by the strong spin−orbit interaction relevant to the heavy lead atoms in $CsPbBr_3$ NCs.[70,71] These features suggest that the gain mechanism in $CsPbBr_3$ NCs may be different from CdSe NCs, which needs more in-depth studies in the future. In this work, with the threshold value of 0.8 mJ cm^{-2}, the average density of excitons per NC ($<N> = \sigma_{TP}F^2/\tau_p$) generated by two-photon excitation is estimated to be 1.6 which is similar to the threshold density of ∼1.5 pumped by single-photon excitation (Figure S7, SI). These facts imply that the multiexciton effect may also be important for the gain generated in $CsPbBr_3$ NCs, which is consistent with the measured pump-fluence dependent TA traces (Figure S6, SI). The exciton dynamics probed at 505 nm with different pump fluences above threshold shows a remarkably shortened lifetime as a clear evidence of Auger recombination due to the multiexciton effect,[72] which can also explain the declined slope of the fluence-dependent emission intensity prior to reaching the threshold (Figure 3B). The involvement of multiexciton effect may also cause the saturation of the ASE intensity under a relatively low fluence (∼1.5 mJ cm^{-2}, Figure 3B) with the exciton density about three times of the threshold value since the two-photon excitation is quadratically dependent on the incident fluence. The lifetime of a biexciton is estimated to be ∼218 ps (Figure S6, SI). The transition energy should be less than that of single exciton due to biexciton binding, which probably explains the red shift of the optical gain with respect to the PL emission. Nevertheless, the possible contribution of single exciton gain cannot be fully excluded at the current stage. For instance, Yukunun et al. reported the optical gain in similar NCs with average excitons of ∼0.5 per NC under one-photon excitation.[45] The lasing in the multiexciton regime observed here may be explained as a consequence of extrinsic losses in $CsPbBr_3$ NCs such as the Urbach tail[45] relevant to imperfections in the crystalline structure.

In summary, we have demonstrated large optical gain and lasing under two-photon excitation in perovskite semiconductor NCs. The superior performance with a remarkably high gain coefficient and low threshold suggests that perovskite semiconductor NCs are particularly suitable for applications in two-photon-pumped lasers arising from the highly efficient PL emission and giant cross section of two-photon absorption. Considering the color tunability and the processability of colloidal gain media,[38,40,44,45] perovskite semiconductor NCs can be coupled into a variety of microresonators to achieve miniaturized lasers covering broad spectral bands for practical applications.[3,7,10,13,58,61,73] The stability has also been regarded as a critical issue facing the optoelectronic devices with perovskite semiconductors. Nevertheless, the two-photon-pumped perovskite NC lasers remain to be active for the time window of ∼10^6 shots in our experiments under ambient environment [Figure S9, SI], which might benefit from the absence of organic cations in the all inorganic NCs used here. The performance may be further improved by engineering the samples with the pump laser coupled into the resonators, since two-photon absorption is quadratically dependent on the local field.

■ ASSOCIATED CONTENT

Supporting Information

The Supporting Information is available free of charge on the ACS Publications website at DOI: 10.1021/jacs.5b12662.

Additional experimental details, characterization of two-photon absorption in the toluene solution of $CsPbBr_3$ NCs, time-resolved PL spectra under one-photon/two-photon excitation, TA characterization of the toluene solution of $CsPbBr_3$ NCs, Auger recombination, single-photon-pumped ASE, laser stability, and control experiments on CdSe/ZnS NCs. (PDF)

■ AUTHOR INFORMATION

Corresponding Authors

*cfzhang@nju.edu.cn
*yuzhang@jlu.edu.cn
*mxiao@uark.edu

Author Contributions

§The authors Y.X. and Q.C. equally contributed to this work.

Notes

The authors declare no competing financial interest.

■ ACKNOWLEDGMENTS

This work is supported by the National Basic Research Program of China (2013CB932903 and 2012CB921801, MOST), the National Science Foundation of China (91233103, 11574140, 11227406 and 11321063), Fundamental Research Funds for the Central Universities, and the Priority Academic Program Development of Jiangsu Higher Education Institutions (PAPD). The authors acknowledge Dr. Xuewei Wu for his technical assistant and Dr. Shiyou Chen for stimulating discussions. C.Z. thanks Dr. Xinyin Cui and Dr. Jiayu Zhang for their help on sample characterizations.

■ REFERENCES

(1) He, G. S.; Tan, L.-S.; Zheng, Q.; Prasad, P. N. *Chem. Rev.* **2008**, *108*, 1245.
(2) He, G. S.; Markowicz, P. P.; Lin, T. C.; Prasad, P. N. *Nature* **2002**, *415*, 767.
(3) Zhang, C.; Zou, C.-L.; Yan, Y.; Hao, R.; Sun, F.-W.; Han, Z.-F.; Zhao, Y. S.; Yao, J. *J. Am. Chem. Soc.* **2011**, *133*, 7276.
(4) Zheng, Q.; Zhu, H.; Chen, S.-C.; Tang, C.; Ma, E.; Chen, X. *Nat. Photonics* **2013**, *7*, 234.
(5) Zhang, C.; Dong, Z. W.; You, G. J.; Qian, S. X.; Deng, H. *Opt. Lett.* **2006**, *31*, 3345.
(6) Zhang, C.; Zhang, F.; Zhu, T.; Cheng, A.; Xu, J.; Zhang, Q.; Mohney, S. E.; Henderson, R. H.; Wang, Y. A. *Opt. Lett.* **2008**, *33*, 2437.
(7) Jasieniak, J. J.; Fortunati, I.; Gardin, S.; Signorini, R.; Bozio, R.; Martucci, A.; Mulvaney, P. *Adv. Mater.* **2008**, *20*, 69.
(8) Xing, G.; Liao, Y.; Wu, X.; Chakrabortty, S.; Liu, X.; Yeow, E. K. L.; Chan, Y.; Sum, T. C. *ACS Nano* **2012**, *6*, 10835.
(9) Wang, Y.; Ta, V. D.; Gao, Y.; He, T. C.; Chen, R.; Mutlugun, E.; Demir, H. V.; Sun, H. D. *Adv. Mater.* **2014**, *26*, 2954.

DOI: 10.1021/jacs.5b12662
J. Am. Chem. Soc. 2016, 138, 3761−3768

(10) Guzelturk, B.; Kelestemur, Y.; Gungor, K.; Yeltik, A.; Akgul, M. Z.; Wang, Y.; Chen, R.; Dang, C.; Sun, H.; Demir, H. V. *Adv. Mater.* **2015**, *27*, 2741.
(11) Olutas, M.; Guzelturk, B.; Kelestemur, Y.; Yeltik, A.; Delikanli, S.; Demir, H. V. *ACS Nano* **2015**, *9*, 5041.
(12) Li, M.; Zhi, M.; Zhu, H.; Wu, W.-Y.; Xu, Q.-H.; Jhon, M. H.; Chan, Y. *Nat. Commun.* **2015**, *6*, 8513.
(13) Bauer, C.; Schnabel, B.; Kley, E. B.; Scherf, U.; Giessen, H.; Mahrt, R. F. *Adv. Mater.* **2002**, *14*, 673.
(14) Cumpston, B. H.; Ananthavel, S. P.; Barlow, S.; Dyer, D. L.; Ehrlich, J. E.; Erskine, L. L.; Heikal, A. A.; Kuebler, S. M.; Lee, I. Y. S.; McCord-Maughon, D.; Qin, J. Q.; Rockel, H.; Rumi, M.; Wu, X. L.; Marder, S. R.; Perry, J. W. *Nature* **1999**, *398*, 51.
(15) Hoover, E. E.; Squier, J. A. *Nat. Photonics* **2013**, *7*, 93.
(16) Xing, J.; Liu, X. F.; Zhang, Q.; Ha, S. T.; Yuan, Y. W.; Shen, C.; Sum, T. C.; Xiong, Q. *Nano Lett.* **2015**, *15*, 4571.
(17) Zhang, C.; Xu, J.; Zhu, T.; Zhang, F.; Tan, Z.; Schiff, S. J.; Su, H.; Gao, S.; Wang, A. Y. *Phys. Rev. B* **2009**, *80*, 035333.
(18) Qu, L. H.; Peng, X. G. *J. Am. Chem. Soc.* **2002**, *124*, 2049.
(19) Resch-Genger, U.; Grabolle, M.; Cavaliere-Jaricot, S.; Nitschke, R.; Nann, T. *Nat. Methods* **2008**, *5*, 763.
(20) Pu, S.-C.; Yang, M.-J.; Hsu, C.-C.; Lai, C.-W.; Hsieh, C.-C.; Lin, S. H.; Cheng, Y.-M.; Chou, P.-T. *Small* **2006**, *2*, 1308.
(21) Stranks, S. D.; Snaith, H. J. *Nat. Nanotechnol.* **2015**, *10*, 391.
(22) Zhou, H.; Chen, Q.; Li, G.; Luo, S.; Song, T.-b.; Duan, H.-S.; Hong, Z.; You, J.; Liu, Y.; Yang, Y. *Science* **2014**, *345*, 542.
(23) Mei, A.; Li, X.; Liu, L.; Ku, Z.; Liu, T.; Rong, Y.; Xu, M.; Hu, M.; Chen, J.; Yang, Y.; Graetzel, M.; Han, H. *Science* **2014**, *345*, 295.
(24) Jeon, N. J.; Noh, J. H.; Kim, Y. C.; Yang, W. S.; Ryu, S.; Il Seol, S. *Nat. Mater.* **2014**, *13*, 897.
(25) Liu, M.; Johnston, M. B.; Snaith, H. J. *Nature* **2013**, *501*, 395.
(26) Burschka, J.; Pellet, N.; Moon, S.-J.; Humphry-Baker, R.; Gao, P.; Nazeeruddin, M. K.; Graetzel, M. *Nature* **2013**, *499*, 316.
(27) Lee, M. M.; Teuscher, J.; Miyasaka, T.; Murakami, T. N.; Snaith, H. J. *Science* **2012**, *338*, 643.
(28) Yakunin, S.; Sytnyk, M.; Kriegner, D.; Shrestha, S.; Richter, M.; Matt, G. J.; Azimi, H.; Brabec, C. J.; Stangl, J.; Kovalenko, M. V.; Heiss, W. *Nat. Photonics* **2015**, *9*, 444.
(29) Shi, D.; Adinolfi, V.; Comin, R.; Yuan, M.; Alarousu, E.; Buin, A.; Chen, Y.; Hoogland, S.; Rothenberger, A.; Katsiev, K.; Losovyj, Y.; Zhang, X.; Dowben, P. A.; Mohammed, O. F.; Sargent, E. H.; Bakr, O. M. *Science* **2015**, *347*, 519.
(30) Dong, Q.; Fang, Y.; Shao, Y.; Mulligan, P.; Qiu, J.; Cao, L.; Huang, J. *Science* **2015**, *347*, 967.
(31) Xing, G.; Mathews, N.; Sun, S.; Lim, S. S.; Lam, Y. M.; Graetzel, M.; Mhaisalkar, S.; Sum, T. C. *Science* **2013**, *342*, 344.
(32) Stranks, S. D.; Eperon, G. E.; Grancini, G.; Menelaou, C.; Alcocer, M. J. P.; Leijtens, T.; Herz, L. M.; Petrozza, A.; Snaith, H. J. *Science* **2013**, *342*, 341.
(33) Deschler, F.; Price, M.; Pathak, S.; Klintberg, L. E.; Jarausch, D.-D.; Higler, R.; Huettner, S.; Leijtens, T.; Stranks, S. D.; Snaith, H. J.; Atatuere, M.; Phillips, R. T.; Friend, R. H. *J. Phys. Chem. Lett.* **2014**, *5*, 1421.
(34) Zhu, H.; Fu, Y.; Meng, F.; Wu, X.; Gong, Z.; Ding, Q.; Gustafsson, M. V.; Trinh, M. T.; Jin, S.; Zhu, X. Y. *Nat. Mater.* **2015**, *14*, 636.
(35) Kim, Y.-H.; Cho, H.; Heo, J. H.; Kim, T.-S.; Myoung, N.; Lee, C.-L.; Im, S. H.; Lee, T.-W. *Adv. Mater.* **2015**, *27*, 1248.
(36) Zhang, Q.; Ha, S. T.; Liu, X.; Sum, T. C.; Xiong, Q. *Nano Lett.* **2014**, *14*, 5995.
(37) Xing, G.; Mathews, N.; Lim, S. S.; Yantara, N.; Liu, X.; Sabba, D.; Gratzel, M.; Mhaisalkar, S.; Sum, T. C. *Nat. Mater.* **2014**, *13*, 476.
(38) Protesescu, L.; Yakunin, S.; Bodnarchuk, M. I.; Krieg, F.; Caputo, R.; Hendon, C. H.; Yang, R. X.; Walsh, A.; Kovalenko, M. V. *Nano Lett.* **2015**, *15*, 3692.
(39) Dou, L.; Wong, A. B.; Yu, Y.; Lai, M.; Kotov, N.; Eaton, S. W.; Fu, A.; Bischak, C. G.; Ma, J.; Ding, T.; Ginsberg, N. S.; Wang, L.-W.; Alivisatos, A. P.; Yang, P. *Science* **2015**, *349*, 1518.
(40) Nedelcu, G.; Protesescu, L.; Yakunin, S.; Bodnarchuk, M. I.; Grotevent, M. J.; Kovalenko, M. V. *Nano Lett.* **2015**, *15*, 5635.
(41) Zhang, F.; Zhong, H.; Chen, C.; Wu, X.-g.; Hu, X.; Huang, H.; Han, J.; Zou, B.; Dong, Y. *ACS Nano* **2015**, *9*, 4533.
(42) Akkerman, Q. A.; D'Innocenzo, V.; Accornero, S.; Scarpellini, A.; Petrozza, A.; Prato, M.; Manna, L. *J. Am. Chem. Soc.* **2015**, *137*, 10276.
(43) Jang, D. M.; Park, K.; Kim, D. H.; Park, J.; Shojaei, F.; Kang, H. S.; Ahn, J.-P.; Lee, J. W.; Song, J. K. *Nano Lett.* **2015**, *15*, 5191.
(44) Wang, Y.; Li, X.; Song, J.; Xiao, L.; Zeng, H.; Sun, H. *Adv. Mater.* **2015**, *27*, 7101.
(45) Yakunin, S.; Protesescu, L.; Krieg, F.; Bodnarchuk, M. I.; Nedelcu, G.; Humer, M.; De Luca, G.; Fiebig, M.; Heiss, W.; Kovalenko, M. V. *Nat. Commun.* **2015**, *6*, 8056.
(46) Zhang, D.; Eaton, S. W.; Yu, Y.; Dou, L.; Yang, P. *J. Am. Chem. Soc.* **2015**, *137*, 9230.
(47) Hassan, Y.; Song, Y.; Pensack, R. D.; Abdelrahman, A. I.; Kobayashi, Y.; Winnik, M. A.; Scholes, G. D. *Adv. Mater.* **2016**, *28*, 566.
(48) Hu, F.; Zhang, H.; Sun, C.; Yin, C.; Lv, B.; Zhang, C.; Yu, W. W.; Wang, X.; Zhang, Y.; Xiao, M. *ACS Nano* **2015**, *9*, 12410.
(49) Zhang, C.; Xu, J.; Zhu, T.; Zhang, F.; Tan, Z.; Schiff, S. J.; Su, H.; Gao, S.; Wang, A. Y. *Phys. Rev. B: Condens. Matter Mater. Phys.* **2009**, *80*, 035333.
(50) Park, Y.-S.; Guo, S.; Makarov, N. S.; Klimov, V. I. *ACS Nano* **2015**, *9*, 10386.
(51) Yamada, Y.; Yamada, T.; Le Quang, P.; Maruyama, N.; Nishimura, H.; Wakamiya, A.; Murata, Y.; Kanemitsu, Y. *J. Am. Chem. Soc.* **2015**, *137*, 10456.
(52) Sheikbahae, M.; Said, A. A.; Wei, T. H.; Hagan, D. J.; Vanstryland, E. W. *IEEE J. Quantum Electron.* **1990**, *26*, 760.
(53) Walters, G.; Sutherland, B. R.; Hoogland, S.; Shi, D.; Comin, R.; Sellan, D. P.; Bake, O. M.; Sargent, E. H. *ACS Nano* **2015**, *9*, 9340.
(54) Klimov, V. I.; Mikhailovsky, A. A.; Xu, S.; Malko, A.; Hollingsworth, J. A.; Leatherdale, C. A.; Eisler, H. J.; Bawendi, M. G. *Science* **2000**, *290*, 314.
(55) Malko, A. V.; Mikhailovsky, A. A.; Petruska, M. A.; Hollingsworth, J. A.; Htoon, H.; Bawendi, M. G.; Klimov, V. I. *Appl. Phys. Lett.* **2002**, *81*, 1303.
(56) Guzelturk, B.; Kelestemur, Y.; Olutas, M.; Delikanli, S.; Demir, H. V. *ACS Nano* **2014**, *8*, 6599.
(57) Grim, J. Q.; Christodoulou, S.; Di Stasio, F.; Krahne, R.; Cingolani, R.; Manna, L.; Moreels, I. *Nat. Nanotechnol.* **2014**, *9*, 891.
(58) Dang, C.; Lee, J.; Breen, C.; Steckel, J. S.; Coe-Sullivan, S.; Nurmikko, A. *Nat. Nanotechnol.* **2012**, *7*, 335.
(59) She, C.; Fedin, I.; Dolzhnikov, D. S.; Demortiere, A.; Schaller, R. D.; Pelton, M.; Talapin, D. V. *Nano Lett.* **2014**, *14*, 2772.
(60) Yeltik, A.; Delikanli, S.; Olutas, M.; Kelestemur, Y.; Guzelturk, B.; Demir, H. V. *J. Phys. Chem. C* **2015**, *119*, 26768.
(61) Wang, Y.; Leck, K. S.; Van Duong, T.; Chen, R.; Nalla, V.; Gao, Y.; He, T.; Demir, H. V.; Sun, H. *Adv. Mater.* **2015**, *27*, 169.
(62) Scott, R.; Achtstein, A. W.; Prudnikau, A.; Antanovich, A.; Christodoulou, S.; Moreels, I.; Artemyev, M.; Woggon, U. *Nano Lett.* **2015**, *15*, 4985.
(63) Eaton, S. W.; Lai, M.; Gibson, N. A.; Wong, A. B.; Dou, L.; Ma, J.; Wang, L.-W.; Leone, S. R.; Yang, P. *Proc. Natl. Acad. Sci. U. S. A.* **2016**, *113*, 1993.
(64) Wang, Y.; Li, X.; Zhao, X.; Xiao, L.; Zeng, H.; Sun, H. *Nano Lett.* **2016**, *16*, 448.
(65) Pan, J.; Sarmah, S. P.; Murali, B.; Dursun, I.; Peng, W.; Parida, M. R.; Liu, J.; Sinatra, L.; Alyami, N.; Zhao, C.; Alarousu, E.; Ng, T. K.; Ooi, B. S.; Bakr, O. M.; Mohammed, O. F. *J. Phys. Chem. Lett.* **2015**, *6*, 5027.
(66) Lo, S. S.; Mirkovic, T.; Chuang, C.-H.; Burda, C.; Scholes, G. D. *Adv. Mater.* **2011**, *23*, 180.
(67) Klimov, V. I.; Ivanov, S. A.; Nanda, J.; Achermann, M.; Bezel, I.; McGuire, J. A.; Piryatinski, A. *Nature* **2007**, *447*, 441.
(68) Huang, L.-y.; Lambrecht, W. R. L. *Phys. Rev. B: Condens. Matter Mater. Phys.* **2013**, *88*, 165203.

DOI: 10.1021/jacs.5b12662
J. Am. Chem. Soc. 2016, 138, 3761−3768

(69) Lang, L.; Yang, J. H.; Liu, H. R.; Xiang, H. J.; Gong, X. G. *Phys. Lett. A* **2014**, *378*, 290.
(70) Zhang, C.; Sun, D.; Sheng, C. X.; Zhai, Y. X.; Mielczarek, K.; Zakhidov, A.; Vardeny, Z. V. *Nat. Phys.* **2015**, *11*, 427.
(71) Giovanni, D.; Ma, H.; Chua, J.; Graetzel, M.; Ramesh, R.; Mhaisalkar, S.; Mathews, N.; Sum, T. C. *Nano Lett.* **2015**, *15*, 1553.
(72) Klimov, V. I.; Mikhailovsky, A. A.; McBranch, D. W.; Leatherdale, C. A.; Bawendi, M. G. *Science* **2000**, *287*, 1011.
(73) Snee, P. T.; Chan, Y. H.; Nocera, D. G.; Bawendi, M. G. *Adv. Mater.* **2005**, *17*, 1131.

DOI: 10.1021/jacs.5b12662
J. Am. Chem. Soc. 2016, 138, 3761−3768